

RSC Advances



This is an *Accepted Manuscript*, which has been through the Royal Society of Chemistry peer review process and has been accepted for publication.

Accepted Manuscripts are published online shortly after acceptance, before technical editing, formatting and proof reading. Using this free service, authors can make their results available to the community, in citable form, before we publish the edited article. This *Accepted Manuscript* will be replaced by the edited, formatted and paginated article as soon as this is available.

You can find more information about *Accepted Manuscripts* in the [Information for Authors](#).

Please note that technical editing may introduce minor changes to the text and/or graphics, which may alter content. The journal's standard [Terms & Conditions](#) and the [Ethical guidelines](#) still apply. In no event shall the Royal Society of Chemistry be held responsible for any errors or omissions in this *Accepted Manuscript* or any consequences arising from the use of any information it contains.



Journal Name

ARTICLE

Study on the interface electronic states of chemically modified ZnO nanowires

Lei Wang,^a Rui Li,^a Lu Feng,^a Jifeng Liu,^{*b} Xuexi Gao,^c and Wenjun Wang^c

Received 00th January 20xx,
Accepted 00th January 20xx

DOI: 10.1039/x0xx00000x

www.rsc.org/

In this work, ZnO nanowires were modified with three mercaptans, respectively. The surface properties of three modified ZnO samples were studied by an experimental and quantum-chemical method. Photoluminescence spectra and electrochemiluminescence spectra were applied to study the surface band gap of modified ZnO nanowires. Electronic-structure calculations that based on the first-principles ultra-soft pseudo-potential approach were applied to study the interface electronic states of ZnO (100) crystal planes that were adsorbed with different mercaptans. The results indicated that thiol number in the mercaptans and the dimension of mercaptans will influence the energy of the conduction band minimum modified ZnO nanowires.

1. Introduction

ZnO nanomaterials modified with thiols have been studied to understand the physical properties of nanomaterials^{1, 2} and applied for the fabrication of new nanodevices.^{3, 4} It has been reported that surface modification of ZnO with thiols may influence the resistive switching effects of diode structures,⁵ and the light absorption, efficient charge separation and transport to electrodes.^{6, 7}

In order to study the effect of functional molecule structure to surface state of modified ZnO nanowires (NWs), three mercaptans that have different thiol number in one molecule and different molecular dimension were used for the surface modification of ZnO NWs. A direct comparison among the surface properties of ZnO NWs modified with three different mercaptans was provided. Fourier transform infrared (FT-IR) spectra and X-ray photoelectron spectra (XPS) were used to study the surface composition. Electrochemiluminescence (ECL) spectra were applied to study the surface band gaps of modified ZnO NWs. Electronic structure calculations based on density functional theory (DFT) were used to study the electron structure of modified ZnO NWs.

2. Experimental Section

2.1 Apparatus

The morphology of obtained ZnO NWs was studied by a FEI Sirion 200 Field Emission Scanning Electron Microscope (FESEM), while the chemical composition of the sample were

measured with an INCA Energy Dispersive Spectrometer (EDS). The phase structure of ZnO NWs was measured with a Bruker D8 advance X-ray diffraction (XRD) with Cu K α ($\lambda=1.5406$ Å) radiation.

The surface modification of ZnO NWs with different mercaptan molecules were characterized by Nicolet 5700 FT-IR spectrometer and an ESCLAB MKII photoelectron spectrometer. For the XPS measurement, binding energies were calibrated by referencing the C 1s peak (284.6 eV) to reduce the sample charge effect. Photoluminescence (PL) spectra were acquired by a FLS 920 fluorescence spectrometer with an excitation wavelength of 325 nm at room temperature.

All electrochemical measurements were conducted on a CHI 760B electrochemical workstation in 0.1M KOH - 0.1M K₂S₂O₈ - 0.1M KCl solution. Ag/AgCl electrode and platinum wire were employed as the reference (RE) and the counter electrodes (CE) respectively. ECL emission intensity was recorded by a RFL-1 ultraweak chemiluminescence analyzer system with the photomultiplier tube biased at 600V.

2.2 Preparation and surface modification of ZnO NWs

ZnO NWs were prepared as reported.^{8, 9} And then the obtained ZnO NWs were modified with mercaptans according to previously reported procedures.¹⁰⁻¹² In brief, the prepared ZnO NWs were firstly dried at 200°C for about 24h, and then 0.15g of the dried ZnO sample was added into 50mL of 95% ethanol solution. After ultrasonic dispersing, the suspended solution was stirred at 65°C for 1h. To this solution, 60mg of mercaptan was added and sonicated for 5min, and stirred for another 1h at 65°C. The obtained products, which were modified with 1-propanethiol, 1,3-propanedithiol and benzylmercaptan, were centrifuged, washed with ethanol, and then dried, respectively.

2.3 Computational details

In order to study the interface electronic states of ZnO NWs modified with different mercaptans, electronic-structure

^a Department of Chemistry, Liaocheng University, Liaocheng 252000, China

^b Key Laboratory of Food Nutrition and Safety, Ministry of Education of China,

Tianjin University of Science and Technology, Tianjin 300457, China. Address here.

^c Department of Physics, Liaocheng University, Liaocheng 252000, China

E-mail: wangl@ustc.edu, liujifeng111@gmail.com

calculations that based on the first-principles ultra-soft pseudo-potential approach were carried out.¹³ The plane wave was based upon the DFT within the Perdew-Burke-Ernzerhof (PBE) form of generalized gradient approximation (GGA) as implemented in the CASTEP package of Materials Studio.¹⁴ The crystal planes (100) model of ZnO were cut out from the wurtzite crystal structure, placed in a $4 \times 2 \times 1$ supercell and separated from its image in the neighbouring supercell by a vacuum region of 15 Å, respectively (Fig 1). A full relaxation of the ionic positions with no symmetry constraints on above three crystal planes was performed. Cutoff energy of 300 eV was used for the atomic relaxation, the energy and electronic property calculations, respectively. In addition, k-point Monkhorst-Pack meshes of $2 \times 2 \times 1$ was adopted for the geometric relaxations and electronic density calculation of the final configuration of crystal planes (100) adsorbed with different mercaptans, respectively. According to the ultrasoft core potentials scheme, the following configurations were used in the valence atomic configuration of adsorbed ZnO: $3d^{10}4s^2$ for zinc, $2s^2 2p^4$ for oxygen and $3s^2 3p^4$ for sulfur.

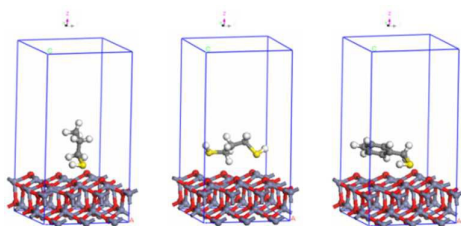


Fig 1 Super cell models of ZnO (100) crystal plane adsorbed with mercaptan molecules. (a) 1-propanethiol, (b) 1,3-propanedithiol and (c) benzylmercaptan.

3. Results and Discussion

3.1 Morphology and structure characterization

FE-SEM image of prepared ZnO NWs was shown in Fig 2a. It was shown that the prepared ZnO NWs were about 5 μm in length and 0.15 μm in diameter. EDS confirms the existence of ZnO (Fig 2b).

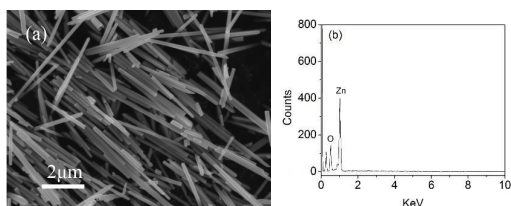


Fig 2 FE-SEM and corresponding EDS of ZnO NWs. (a) FE-SEM, (b) EDS.

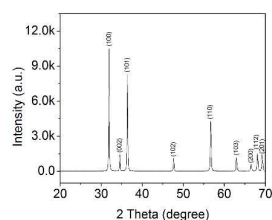


Fig 3 XRD patterns of prepared ZnO NWs.

The XRD pattern of obtained ZnO NWs was shown in Fig 3. All the diffraction peaks in the pattern match well with the standard pattern of hexagonal wurtzite-structure ZnO (JCPDS NO. 36-1451)⁸.

3.2 FT-IR measurement of modified ZnO NWs

FT-IR spectrum has previously been used to probe the interactions between small molecules and mineral surfaces,¹⁵ the nature of the surface modification of ZnO can be investigated and interpreted on the basis of the anchoring of organic ligands onto the surface of oxides.¹⁶⁻²⁰ It has been reported that the characteristic stretching of Zn-O bonds in zinc oxide can be observed below 600 cm^{-1} .^{12, 21} The FT-IR spectra of ZnO NWs modified with 1-propanethiol, 1,3-propanedithiol and benzylmercaptan were shown in Fig 4.

For ZnO NWs modified with 1-propanethiol (Fig 4a), the strong adsorption peaks at 2959 cm^{-1} , 2869 cm^{-1} and 1374 cm^{-1} came from the asymmetric stretching vibration, symmetrical stretching vibration and the scissoring vibration of the terminal methyl group, while the strong peak present at 2929 cm^{-1} and the medium peak at 1459 cm^{-1} could be contributed to the asymmetric stretching vibration and the scissoring vibration of methylene groups in functional 1-propanethiol molecules respectively. The medium peaks appeared at 1292, 1239, 1091, 1052, 895 cm^{-1} and the weak peak at 782 cm^{-1} came from the stretching vibration and the scissoring vibration of C-S bonds.

For ZnO NWs modified with 1,3-propanedithiol (Fig 4b), the strong peak present at 2923 cm^{-1} , the medium peak at 2850 cm^{-1} and the medium peak at 1439 cm^{-1} could be contributed to the asymmetric stretching vibration, symmetrical stretching vibration, and the scissoring vibration of methylene groups, respectively. The weak peak appeared at 1291 cm^{-1} and the medium peak at 1238 cm^{-1} came from the stretching vibration of C-S bonds of attached 1,3-propanedithiol.

For ZnO NWs modified with benzylmercaptan (Fig 4c), the strong peak present at 2931 cm^{-1} and the medium peak at 1452 cm^{-1} resulted from the asymmetric stretching vibration and the scissoring vibration of methylene groups, respectively. The peak at 1600 cm^{-1} originate from the stretching vibration of C=C skeleton in the benzene ring, the peaks at 758 and 698 cm^{-1} could be associated with the deformation vibration of C-H in mono-substituted aromatic hydrocarbons. The medium peaks appeared at 1251, 1073 and 1028 cm^{-1} came from the stretching vibration and the scissoring vibration of C-S bonds of benzylmercaptan bonded onto the surface of ZnO NWs.

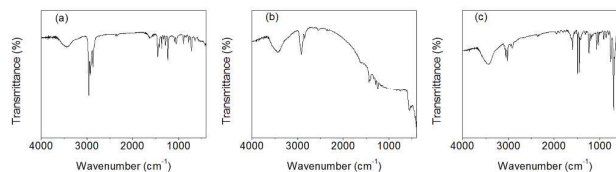


Fig 4 FT-IR spectra of ZnO NWs modified with different mercaptan molecules. (a) 1-propanethiol, (b) 1,3-propanedithiol, and (c) benzylmercaptan.

3.3 XPS measurement of modified ZnO NWs

The electronic structures and surface compositions of obtained ZnO samples were determined by XPS.

The Zn 2p 3/2 XPS spectra of ZnO NWs modified with 1-propanethiol, 1,3-propanedithiol and benzylmercaptan were shown in Fig 5. The peaks of above three samples were centered at 1021.2 eV, which is smaller than the 1021.49 eV of the Zn 2p XPS peak of crystal lattice zinc from ZnO.^{8, 22, 23} The decrease of Zn binding energy indicated the formation of Zn-S bond on the surface of ZnO NWs.

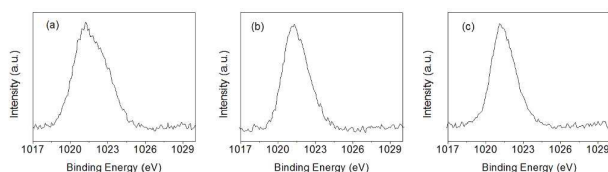


Fig 5 Zn 2p XPS spectra of ZnO NWs modified with different mercaptan molecules. (a) 1-propanethiol, (b) 1,3-propanedithiol, and (c) benzylmercaptan.

The O 1s XPS spectra of modified ZnO NWs were shown in Fig 6. The peak centred at 531.5eV is associated with O²⁻ ions in oxygen-deficient regions within the matrix of ZnO, the large atomic percentage of oxygen-deficient may involve the breakage of Zn-O bond and the formation of Zn-S complexes on the surface of ZnO NWs in the process of surface modification, which means that the surface composition of ZnO NWs were changed after surface modification.

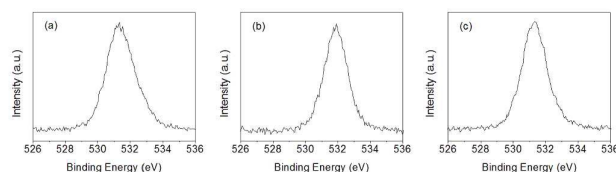


Fig 6 O 1s XPS spectra of ZnO NWs modified with different mercaptan molecules. (a) 1-propanethiol, (b) 1,3-propanedithiol, and (c) benzylmercaptan.

The S 2p XPS spectra of obtained ZnO samples were measured (Fig 7). The strong peaks centred at 162.8 eV is in accord with the Zn-S covalent bond signal in literatures.^{11, 24, 25}

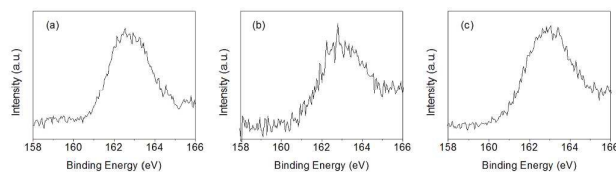


Fig 7 S 2p XPS spectra of ZnO NWs modified with different mercaptan molecules. (a) 1-propanethiol, (b) 1,3-propanedithiol, and (c) benzylmercaptan.

Although the adsorption mechanism of thiols on O rich ZnO surfaces has been interpreted by O-S attachment mode,²⁶ the S 2p XPS spectra in this work indicated that 1-propanethiol, 1,3-propanedithiol and benzylmercaptan were attached onto the surface of ZnO NWs by the formation of Zn-S complexes.

3.4 PL measurement of modified ZnO NWs

The optical properties of modified ZnO were investigated by PL measurements at room temperature, as shown in Fig 8.

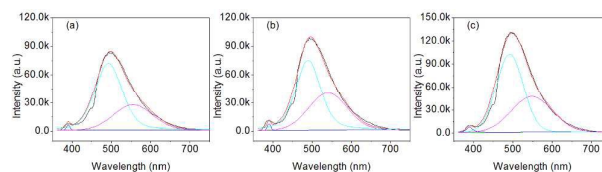


Fig 8 PL spectra of ZnO NWs modified with different mercaptan molecules. (a) 1-propanethiol, (b) 1,3-propanedithiol, and (c) benzylmercaptan.

The PL spectrum of ZnO NWs modified with 1-propanethiol can be decomposed into three Gaussian components centred in 390nm, 495nm, and 555 nm. The relative percentage of above peaks was 0.6%, 68.9% and 30.5% respectively (Fig 8a). However, for the PL spectrum of ZnO NWs modified with 1,3-propanedithiol, three Gaussian components centred in 390nm, 490nm, and 540 nm by can be decomposed. The relative percentage of above peaks was 0.6%, 59.0% and 40.4% respectively (Fig 8b). While three Gaussian components centred in 390nm, 492nm, and 548 nm can be obtained for PL spectrum of ZnO NWs modified with benzylmercaptan. The relative percentage of above peaks was 1.3%, 58.9% and 39.8% respectively (Fig 8c). The results indicated that the green emission band in PL spectrum of ZnO sample may be influenced by the thiol number in the mercaptan molecule and the molecular dimension.

3.5 ECL measurement of modified ZnO NWs

In ECL measurements, 2.0 μ L of 1 mg mL⁻¹ well-dispersed modified ZnO samples was dropped onto the electric surface of ITO and then used as working electrode (WE). Cyclic voltammetry with the potential scan region of 0 to -2.0 V was used to display the ECL emission intensity. It was shown that ZnO NWs modified with different mercaptans present stable ECL signals in 1500s (Fig 9).

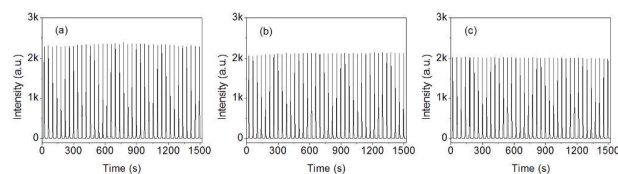


Fig 9 ECL emission of ZnO NWs modified with different mercaptan molecules. (a) 1-propanethiol, (b) 1,3-propanedithiol, and (c) benzylmercaptan.

ECL spectra can be use to characterize the surface energy levels of ZnO samples.^{9, 27} As chronocoulometry was applied to the WE, ECL spectra were recorded by a FLS 920 fluorescence spectrometer with emission scan mode, as shown in Fig 10. The results indicated that the maximum ECL wavelengths were 631 nm for ZnO NWs modified with 1-propanethiol, 607 nm for ZnO NWs treated with 1,3-propanedithiol, and 613 nm for ZnO NWs modified with benzylmercaptan. The variation of ECL maximum wavelength reflected the change of surface state of modified ZnO NWs. For 1-propanethiol molecule, only one -SH can be bound to the surface ZnO, while two -SH in the 1,3-

propanedithiol molecule can be bound to two surface Zn atoms. For benzylmercaptan, the large molecular dimension may influence the degree of surface modification.

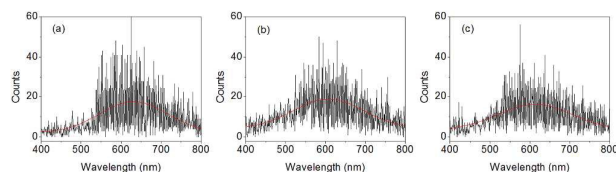


Fig 10 ECL spectra of ZnO NWs modified with different mercaptan molecules. (a) 1-propanethiol, (b) 1,3-propanedithiol, and (c) benzylmercaptan.

3.6 Theoretical study of modified ZnO NWs

In the theoretical chemical calculation, electron density difference can be used to study the charge transfer. The charge density difference of ZnO (100) crystal plane adsorbed with different mercaptans was shown in Fig 11. The red region between Zn atom on the ZnO (100) crystal plane and S atom in the mercaptan molecule reflected the increase of electron cloud density, while the blue regions around Zn atom and S atom indicated that the electron cloud density decreased as mercaptan molecule was adsorbed onto the ZnO (100) crystal plane. The increase of electron cloud density between Zn atom and S atom demonstrated the formation of Zn-S bond as mercaptan was adsorbed onto the ZnO (100) crystal plane.

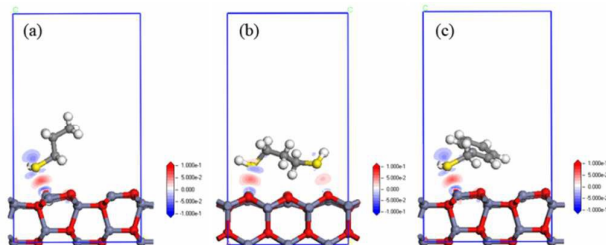


Fig 11 The charge density difference of ZnO (100) crystal planes adsorbed with different mercaptan molecules. (a) 1-propanethiol (b) 1,3-propanedithiol; (c) benzylmercaptan.

The band structures and density of states of ZnO (100) crystal planes adsorbed with mercaptan were calculated by theoretical quantum-chemical DFT methods, as shown in Fig 12. The band gaps for the ZnO crystal planes (100) adsorbed with 1-propanethiol, 1,3-propanedithiol and benzylmercaptan were 0.843, 0.876 and 0.859 eV, respectively.

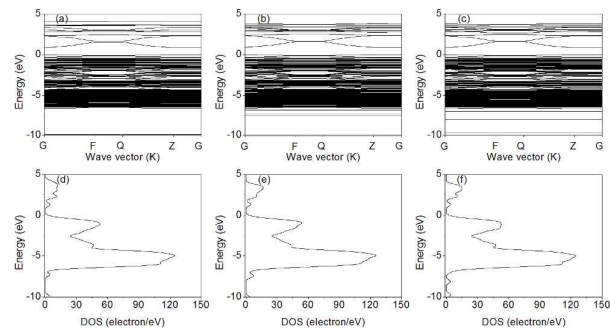


Fig 12 Band structures and corresponding density of states of ZnO (100) crystal planes adsorbed with different mercaptan molecules. (a) and (d) 1-propanethiol; (b) and (e) 1,3-propanedithiol; (c) and (f) benzylmercaptan.

The calculated band gap of ZnO (100) crystal plane adsorbed with different mercaptan is smaller than that obtained from ECL measurement. It is an universal problem to underestimate the band gap in the theoretical chemical calculation by GGA/LDA,²⁸ which can be attributed to the well known intrinsic factor of DFT.²⁹ The underestimation of the band gap might result from the overestimation of the energy of Zn 3d that gave rise to the increase of the interaction energy among Zn 3d, O 2p and S 3p, which led to the broadening of the valence bandwidth and the decrease of the band gap.³⁰⁻³² However, the underestimation will not influence the theoretical analysis of the electronic structure of ZnO nanostructures.^{30, 33}

In order to obtain further insight into the effects of attached molecular structure on the interface electronic states of ZnO samples, the partial electronic densities of states were used to analyze the electronic properties of ZnO (100) crystal planes adsorbed with different mercaptan molecules (Fig 13).

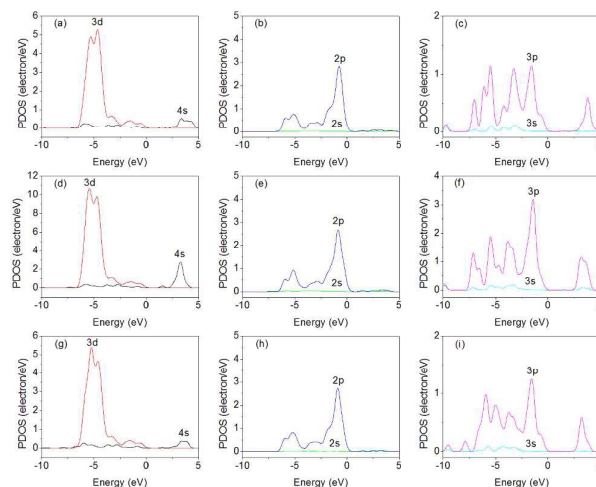


Fig 13 Partial electronic densities of states of Zn atom, O atom and S atom on different ZnO (100) crystal planes adsorbed with different mercaptan molecules. (a), (b) and (c) 1-propanethiol; (d), (e) and (f) 1,3-propanedithiol; (g), (h) and (i) benzylmercaptan.

When mercaptan molecules were attached onto the surface of ZnO, S atoms are cooperated with Zn atoms, the valence band maximum states come mainly from the S 3p and O 2p, whereas the conduction band minimum states are based on the S 3p and Zn 4s states. The valence band maximum energy of ZnO (100) crystal plane adsorbed with 1-propanethiol is almost equivalent to that in ZnO (100) crystal plane adsorbed with 1,3-propanedithiol and benzylmercaptan, while the conduction band bottom energy increased as the adsorbed molecule changed from 1-propanethiol, benzylmercaptan to 1,3-propanedithiol. Theoretical study has verified that hybridization between Zn 4s orbits with S 3p orbits induces charge redistribution, which causes the 2p electrons in O and 3p electrons in S sites to become spin-polarized.³⁴ The higher

energy of the conduction band bottom of the (100) crystal plane adsorbed with 1,3-propanedithiol may originated from the formation of coordination complexes between two –SH and surface Zn atoms. The conduction band minimum in the (100) crystal plane adsorbed with benzylmercaptan shifted to higher energy direction compared with that in the (100) crystal plane adsorbed with 1-propanethiol, which may be related to the steric repulsion between the molecules. So the band gap (100) crystal plane increased as the adsorbed mercaptan molecules changed from 1-propanethiol, benzylmercaptan to 1,3-propanedithiol. The trend of band gap variation obtained by theoretical computation is almost the same to that achieved by analyzing the ECL spectra for modified ZnO NWs. So it demonstrated that the interface electronic states of ZnO samples were influenced by the surface molecular structures.

Conclusion

In this work, three mercaptan molecules were used to study the effect of functional molecule structure to surface state of modified ZnO NWs. The experimental and quantum-chemical results indicated the variation of surface band gaps may originate from the difference of charge redistribution in the surface of ZnO NWs anchored with mercaptan molecule.

Acknowledgments

This work was supported by the National Natural Science Foundation of China (Grant No. 21127006, 21205056, 61275147), Natural Science Foundation of Shandong Province (ZR2012BM007). We also acknowledge the National Super Computing Center in Jinan for providing computational resources.

References

- 1 A. McLaren, T. Valdes-Solis, G. Li and S. C. Tsang, *J. Am. Chem. Soc.*, 2009, 131, 12540-12541.
- 2 L. Wang, L. Feng and J. Liu, *RSC Adv.*, 2014, 4, 62505-62510.
- 3 Q. H. Li, T. Gao, Y. G. Wang and T. H. Wang, *Appl. Phys. Lett.*, 2005, 86, 123117.
- 4 Z. Wang, Y. Zhao, D. Schiferl, C. S. Zha and R. T. Downs, *Appl. Phys. Lett.*, 2004, 85, 124-126.
- 5 F. Verbakel, S. C. J. Meskers and R. A. J. Janssen, *J. Phys. Chem. C*, 2007, 111, 10150-10153.
- 6 S. P. Garcia and S. Semancik, *Chem. Mater.*, 2007, 19, 4016-4022.
- 7 M. Grätzel, *Acc. Chem. Res.*, 2009, 42, 1788-1798.
- 8 X. G. Han, H. Z. He, Q. Kuang, X. Zhou, X. H. Zhang, T. Xu, Z. X. Xie and L. S. Zheng, *J. Phys. Chem. C*, 2009, 113, 584-589.
- 9 L. Wang, Q. Yue, H. Li, S. Xu, L. Guo, X. Zhang, H. Wang, X. Gao, W. Wang, J. Liu and P. Liu, *Sci. China: Chem.*, 2013, 56, 86-92.
- 10 J.-H. Koo, J.-J. Cho, J.-H. Yang, P.-J. Yoo, K.-W. Oh and J.-H. Park, *Bull. Korean Chem. Soc.*, 2012, 33, 636-640.
- 11 J. Singh, J. Im, J. E. Whitten, J. W. Soares and D. M. Steeves, *Langmuir*, 2009, 25, 9947-9953.
- 12 S.-Z. Deng, H.-M. Fan, M. Wang, M.-R. Zheng, J.-B. Yi, R.-Q. Wu, H.-R. Tan, C.-H. Sow, J. Ding, Y.-P. Feng and K.-P. Loh, *ACS Nano*, 2010, 4, 495-505.
- 13 D. Vanderbilt, *Phys. Rev. B*, 1990, 41, 7892-7895.
- 14 J. Perdew, K. Burke and M. Ernzerhof, *Phys. Rev. Lett.*, 1996, 77, 3865-3868.
- 15 N. J. Nicholas, G. V. Franks and W. A. Ducker, *Langmuir*, 2012, 28, 7189-7196.
- 16 S. Sakohara, M. Ishida and M. A. Anderson, *J. Phys. Chem. B*, 1998, 102, 10169-10175.
- 17 S. Sakohara, L. D. Tickanan and M. A. Anderson, *J. Phys. Chem.*, 1992, 96, 11086-11091.
- 18 M. Nara, H. Torii and M. Tasumi, *J. Phys. Chem.*, 1996, 100, 19812-19817.
- 19 P. J. Thistlethwaite, M. L. Gee and D. Wilson, *Langmuir*, 1996, 12, 6487-6491.
- 20 P. J. Thistlethwaite and M. S. Hook, *Langmuir*, 2000, 16, 4993-4998.
- 21 P. D. Cozzoli, A. Kornowski and H. Weller, *J. Phys. Chem. B*, 2005, 109, 2638-2644.
- 22 Z. G. Wang, X. T. Zu, S. Zhu and L. M. Wang, *Physica E*, 2006, 35, 199-202.
- 23 Y. Zhang, G. Du, X. Wang, W. Li, X. Yang, Y. Ma, B. Zhao, H. Yang, D. Liu and S. Yang, *J. Cryst. Growth*, 2003, 252, 180-183.
- 24 J. Singh and J. E. Whitten, *J. Phys. Chem. C*, 2008, 112, 19088-19096.
- 25 E. M. Barea, R. Caballero, L. López-Arroyo, A. Guerrero, P. de la Cruz, F. Langa and J. Bisquert, *ChemPhysChem*, 2011, 12, 961-965.
- 26 P. W. Sadik, S. J. Pearton, D. P. Norton, E. Lambers and F. Ren, *J. Appl. Phys.*, 2007, 101, 104514.
- 27 L. Wang, Q. Yue, H. Li, S. Xu and J. Liu, *Phys. Chem. Chem. Phys.*, 2013, 15, 9058-9061.
- 28 S. H. Wei and A. Zunger, *Phys. Rev. B*, 1988, 37, 8958-8981.
- 29 L. Li, W. Wang, H. Liu, X. Liu, Q. Song and S. Ren, *J. Phys. Chem. C*, 2009, 113, 8460-8464.
- 30 D. Vogel, P. Krüger and J. Pollmann, *Phys. Rev. B*, 1995, 52, R14316-R14319.
- 31 P. Schröer, P. Krüger and J. Pollmann, *Phys. Rev. B*, 1994, 49, 17092-17101.
- 32 S. Sapra, N. Shanthi and D. D. Sarma, *Phys. Rev. B*, 2002, 66, 205202.
- 33 P. Schröer, P. Krüger and J. Pollmann, *Phys. Rev. B*, 1993, 47, 6971-6980.
- 34 Q. Wang, Q. Sun and P. Jena, *J. Chem. Phys.*, 2008, 129, 164714.